

Enzyme Ligands

International Edition: DOI: 10.1002/anie.201509843
German Edition: DOI: 10.1002/ange.201509843

Structure-Based Development of an Affinity Probe for Sirtuin 2

Matthias Schiedel, Tobias Rumpf, Berin Karaman, Attila Lehotzky, Stefan Gerhardt, Judit Ovádi, Wolfgang Sippl, Oliver Einsle, and Manfred Jung*

Abstract: Sirtuins are NAD^+ -dependent protein deacylases that cleave off acetyl groups, as well as other acyl groups, from the ϵ -amino group of lysines in histones and other substrate proteins. Dysregulation of human Sirt2 activity has been associated with the pathogenesis of cancer, inflammation, and neurodegeneration, thus making Sirt2 a promising target for pharmaceutical intervention. Here, based on a crystal structure of Sirt2 in complex with an optimized sirtuin rearranging ligand (SirReal) that shows improved potency, water solubility, and cellular efficacy, we present the development of the first Sirt2-selective affinity probe. A slow dissociation of the probe/enzyme complex offers new applications for SirReals, such as biophysical characterization, fragment-based screening, and affinity pull-down assays. This possibility makes the SirReal probe an important tool for studying sirtuin biology.

NAD^+ -dependent protein deacylases, also termed sirtuins, were initially described as class III histone deacetylases (HDACs).^[1] However, a multitude of non-histone substrates such as p53,^[2] NF κ B,^[3] α -tubulin,^[4] and BubR1^[5] have been discovered in recent years. Besides $N\epsilon$ -deacetylation of lysine residues, sirtuins have been shown to catalyze further post-translational modifications, including demyristoylation,^[6] desuccinylation,^[7] and ADP-ribosylation.^[8] By interacting with their substrate proteins, sirtuins have been implicated as influencing a wide range of cellular processes such as apoptosis, regulation of mitosis, inflammation, ageing, and metabolic sensing. The human genome encodes seven different sirtuin isotypes, which differ in their subcellular localization and their catalytic activity.^[9] The human isotype

sirtuin 2 (Sirt2) is both a nuclear and a cytoplasmic protein. By deacetylating its substrate proteins, Sirt2 acts as a major regulator of the cell cycle,^[4] autophagy,^[10] and peripheral myelination,^[11] as well as being a suppressor of inflammation in the brain.^[12] The involvement of Sirt2 in tumorigenesis is an ongoing controversial debate. Generally considered as a tumor suppressor in some types of cancer,^[13] Sirt2 was also shown to exert the opposite role of a promoter of tumor growth.^[14] Furthermore, Sirt2-mediated deacetylation of H3K18Ac was reported to play a critical role during bacterial infection by reprogramming the transcription of host cells.^[15] Bearing in mind the variety of Sirt2 substrates and the downstream signaling effects, it is apparent that Sirt2 inhibitors are urgently needed to further validate the potential of Sirt2 as a drug target to fight cancer, inflammation, and neurodegenerative diseases. Although a number of highly potent Sirt2 inhibitors have been discovered recently (see Figure S1 in the Supporting Information),^[16] to date there is no targeted inhibitor of Sirt2 that has reached clinical trials. Potent, isotype-selective, and druglike modulators of Sirt2 activity with proven cellular target engagement are still scarce. Recently, we discovered a novel class of potent and highly selective Sirt2 inhibitors, the sirtuin rearranging ligands (SirReals; Figure 1).^[17]

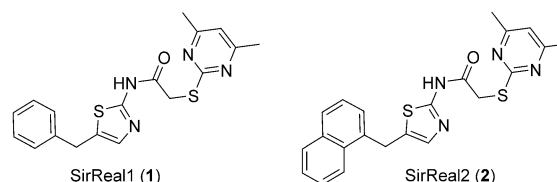


Figure 1. Chemical structures of Sirt2 inhibitors SirReal1 (1) and SirReal2 (2).

Upon binding, these inhibitors induce a major rearrangement of the Sirt2 active site and open up a so far unexploited binding pocket. This unique rearrangement is the basis for the high potency and, particularly, the excellent isotype selectivity of the SirReals. This pocket was, therefore, termed the “selectivity pocket”. SirReal2 (2), with an IC_{50} value of 0.4 μ M and remarkable isotype selectivity, is the most promising agent among the first generation SirReals.^[17] For further characterization of this inhibitor class and to transfer the unique features of SirReals to new applications, and allow us to gain deeper insights into sirtuin biology, we decided to design an affinity probe for Sirt2. This process was guided by the structural insights obtained from Sirt2–SirReal complexes. To access the Sirt2-bound SirReal without losing the affinity and selectivity of the ligand, we aimed to exploit the

[*] M. Schiedel, Dr. T. Rumpf, Prof. Dr. M. Jung
Institut für Pharmazeutische Wissenschaften
Albert-Ludwigs-Universität Freiburg
Albertstrasse 25, 79104 Freiburg im Breisgau (Germany)
E-mail: manfred.jung@pharmazie.uni-freiburg.de

Dr. S. Gerhardt, Prof. Dr. O. Einsle
Institute für Biochemie und BIOS Centre for Biological
Signaling Studies
Albert-Ludwigs-Universität Freiburg
Albertstrasse 21, 79104 Freiburg im Breisgau (Germany)

B. Karaman, Prof. Dr. W. Sippl
Institute für Pharmazie
Martin-Luther-Universität Halle-Wittenberg
Wolfgang-Langenbeck-Strasse 4, 06120 Halle, Saale (Germany)

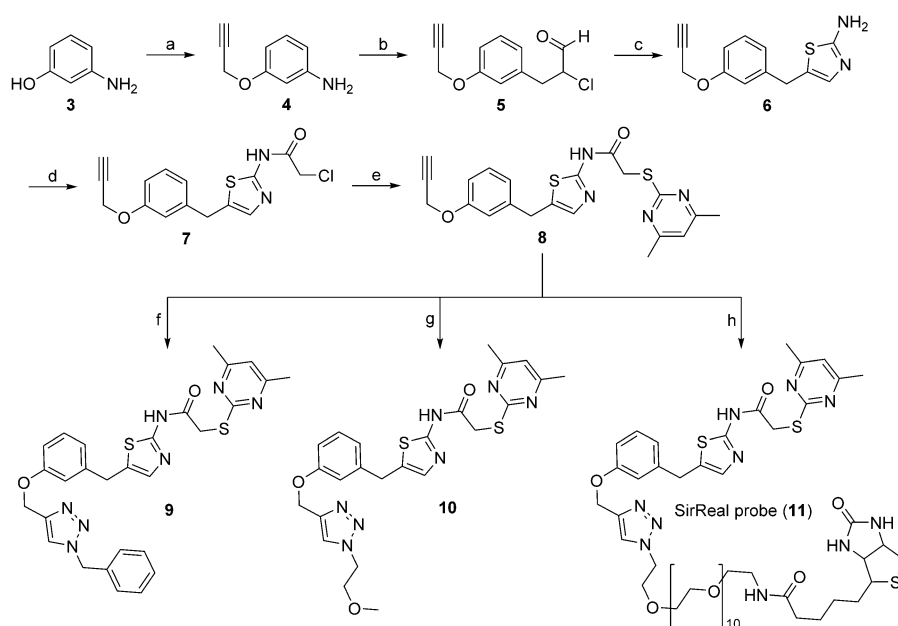
Dr. A. Lehotzky, Prof. Dr. J. Ovádi
Institute of Enzymology, Research Centre for Natural Sciences
Hungarian Academy of Sciences
Magyar Tudósok körútja 2, H-1117 Budapest (Hungary)

Supporting information and ORCID(s) from the author(s) for this article are available on the WWW under <http://dx.doi.org/10.1002/anie.201509843>.

acyllysine substrate channel leading from the active site of Sirt2 to the protein surface. As the methylaryl moieties of SirReals extend towards the acyllysine channel,^[17] we decided to connect a PEG linker carrying the biotin label to this site of the inhibitor. This would address the lysine tunnel and allow the inhibitor to be coupled to an affinity matrix without disturbing the inhibition. Guided by molecular docking, which revealed that larger substituents at the naphthyl moiety of the more potent SirReal2 (**2**) would lead to a steric clash, we selected the benzyl derivative SirReal1 (**1**) as the ideal starting point for the probe design (Figure S2).

To validate our probe design, two new SirReals (**9**, **10**) (Scheme 1) were prepared by adapting our previously described synthesis of SirReal1 (**1**)^[17] for available Sirt2–SirReal structures. The first step was the propargylation of 3-aminophenol (**3**) followed by a Meerwein reaction to generate compound **5**.^[18] Condensation of the resulting α -chloropropenal **5** with thiourea furnished the aminothiazole scaffold **6**.^[18b] The aminothiazole was then chloroacetylated to obtain compound **7**, and a subsequent nucleophilic substitution with dimethylmercaptopyrimidine generated compound **8**.^[19] Finally, compound **8** was functionalized through a Cu-catalyzed Huisgen cycloaddition to yield **9**, **10**, and, eventually, the SirReal probe (**11**).^[20]

A homogeneous fluorescence-based Sirt2 activity assay^[21] led to the triazoles **9** and **10** being characterized as new Sirt2 inhibitors (Table 1) that are more than 20 times more potent than the parent inhibitor SirReal1 (**1**).



Scheme 1. Synthesis of **9**, **10**, and the SirReal probe (**11**). Reagents and conditions: a) propargyl bromide, NaOH, acetonitrile, 20 °C, 12 h, 75% yield; b) NaNO₂, HCl, water, 0 °C, 20 min; then acrolein, CuCl₂·2H₂O, acetone, 20 °C, 3 h; c) thiourea, ethanol, reflux, 2 h, 18% yield over two steps; d) chloroacetyl chloride, DIPEA, acetonitrile, 20 °C, 2 h, 99% yield; e) 4,6-dimethyl-2-methylsulfanylpuridine, Na₂CO₃, KI, DMSO, 20 °C, 2 h, 76% yield; f) benzyl azide, sodium ascorbate, CuSO₄, TBTA, water/*t*BuOH/DMF (1:1:1), 20 °C, 12 h, 72% yield; g) 1-azido-2-methoxyethane, sodium ascorbate, CuSO₄, TBTA, water/*t*BuOH/DMF (1:1:1), 20 °C, 12 h, 50% yield; h) azido/PEG11/biotin conjugate, sodium ascorbate, CuSO₄, TBTA, water/*t*BuOH/DMF (1:1:1), 20 °C, 12 h, 37% yield. DIPEA = *N,N*-diisopropylethylamine, TBTA = tris(benzyltriazolylmethyl)amine.

Table 1: IC₅₀ values of the second generation SirReals (**9**, **10**), SirReal probe (**11**), as well as SirReal1 and SirReal2 (**1**, **2**) as references.

Compound	Sirt1 IC ₅₀ [μM]	Sirt2 IC ₅₀ [μM]	Sirt3 IC ₅₀ [μM]
1	> 100	3.745 ± 0.831	> 100
2	> 100	0.435 ± 0.083	> 100
9	> 100	0.163 ± 0.014	> 100
10	> 100	0.118 ± 0.006	> 100
11	> 100	0.305 ± 0.111	> 100

Besides an improved potency, these second generation SirReals have enhanced water solubility, while retaining the unique isotype selectivity of the first generation SirReals (Table 1). We were able to obtain a crystal structure of Sirt2 in complex with **9**, which nicely confirmed the proposed binding mode (PDB-ID 5DY5). Triazole **9** binds to Sirt2 in a similar fashion as the previously reported SirReal1 and SirReal2.^[17] The benzyloxy moiety is slightly twisted relative to the conformation of the benzyl moiety of SirReal1 in complex with Sirt2. Indeed, the triazole, as well as the terminal benzyl group, further extend into the acyllysine binding site and block the substrate binding site more effectively than SirReal1 and SirReal2. Additionally, the triazole forms hydrogen bonds with Arg97 of the cofactor binding loop (Figure 2 and Figure S3). We could also see that the N substituent of the triazole moiety points towards the entry of the acyllysine channel, so we could continue to pursue the synthesis of the probe in the proposed manner.

To prove that the extended binding interaction with the acyllysine channel and its more efficient blockage is also relevant under physiological conditions, we assessed the cellular activity of **9** and **10** by using immunofluorescence microscopy. Enhanced tubulin hyperacetylation was found compared to the prior lead structure SirReal2 (**2**; Figure S4), which is probably a result of both increased potency and aqueous solubility. Thus, we performed the synthesis of the SirReal probe (**11**) by using a pegylated biotin with a terminal azide function (Scheme 1). We determined an IC₅₀ value of 0.3 μM for our probe by using a homogeneous fluorescence-based activity assay.^[21] For further biophysical characterization we used biolayer interferometry, which enabled us to trace the interaction between the surface-bound SirReal probe and Sirt2 as a shift in the interference pattern of the incident light. We were able to show a dose-dependent binding of Sirt2 to the immobilized SirReal probe and determined rate constants of $k_{on} = 6.89 \pm 0.22 \times 10^3 \text{ M}^{-1} \text{ s}^{-1}$ and $k_{off} =$

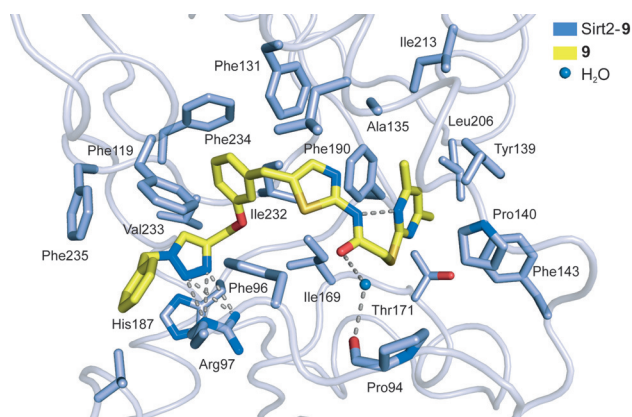


Figure 2. Crystal structure of the Sirt2–9 complex. **9** is shown in yellow sticks, the interacting residues are represented as light blue sticks. Hydrogen bonds are shown as dashed gray lines and water molecules are shown as blue spheres.

$6.99 \pm 0.31 \times 10^{-4} \text{ s}^{-1}$, which result in a K_D value of $0.1 \mu\text{M}$ (Figure 3a). The linearity of the binding ($r^2 = 0.9774$) is indicated in Figure S5. The previously mentioned “selectivity pocket” is formed by two loops of the hinge region, which connects the Rossmann fold domain with the zinc-binding domain. During catalysis, Sirt2 undergoes a conformational change, which brings the domains into proximity. The binding of SirReals to the Sirt2 active site blocks this process by locking Sirt2 in an open conformation.^[17] Our kinetic measurements, which reveal very slow dissociation kinetics, show that Sirt2 traps the bound ligand in its active site as a consequence of its conformational adaptation upon binding the ligand. This induces a long residence time of the ligand and causes slow dissociation (see Figure 3a).^[22] In contrast to a previously described sirtuin affinity probe,^[23] our SirReal probe shows excellent isotype selectivity (Figure 3b). To validate the proposed binding mode of the probe, we preincubated Sirt2 with different potential competitors before exposing it to the immobilized SirReal probe. We observed competition of the SirReal probe with NAD^+ , an oligopeptide containing unlabeled acetyllysine, ADPR, and SirReal2 (Figure 3c). These results are in line with the kinetics of SirReal1-mediated inhibition.^[17] As a negative control, we used nicotinamide, the physiological inhibitor of sirtuin activity, which exhibited no competition with the SirReal probe. This finding is supported by our previous structural studies that revealed that Sirt2 can bind SirReals and nicotinamide simultaneously. To demonstrate the suitability of our SirReal probe for further applications, we performed proof-of-concept studies for fragment-based drug design (FBDD) and affinity pull-down experiments. As a result of the low affinity of fragments to target enzymes, fragment screening is routinely performed at very high concentrations, thus limiting the application of biochemical activity assays based on spectroscopic methods, for example, fluorescence and UV/Vis spectroscopy.^[24] Biophysical methods such as biolayer interferometry are less prone to assay interferences and are, therefore, ideal for fragment screening.^[25] To validate the suitability of the SirReal probe in combination with biolayer interferometry for fragment

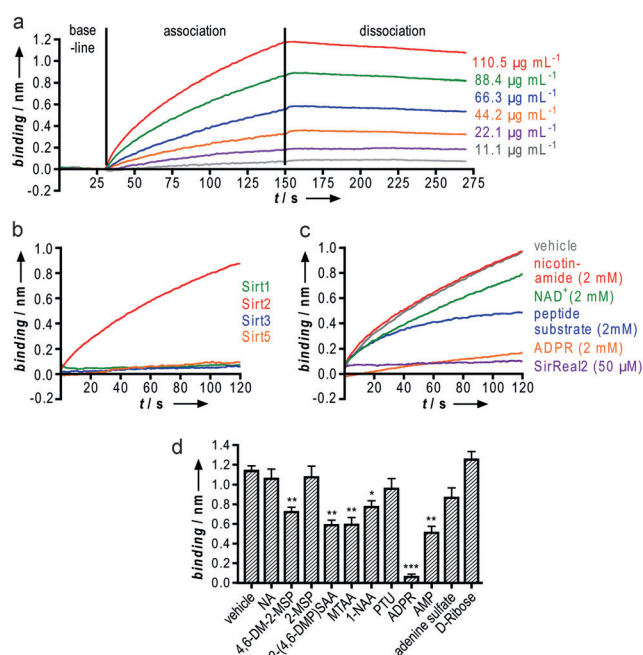


Figure 3. Biophysical characterization of the SirReal probe (**11**) by using biolayer interferometry. a) Representative biolayer interferometry sensorgrams showing different concentrations of Sirt2 binding to immobilized **11**. b) Representative biolayer interferometry sensorgrams (only the association phase is shown) of different sirtuin isotypes ($1.7 \mu\text{M}$) binding to immobilized **11**. c) Representative biolayer interferometry sensorgrams (only the association phase is shown) of Sirt2 ($110.5 \mu\text{g mL}^{-1}$) binding to immobilized **11** after preincubation with potential competitors. d) Shift [nm] detected at the end of the association phase after preincubation of Sirt2 ($110.5 \mu\text{g mL}^{-1}$) with the given ligands and ligand fragments (5 mM , see Figure S6 for structures). NA = nicotinamide, 4,6-DM-2-MSP = 4,6-dimethyl-2-methylsulfanylpyrimidine, 2-MSP = 2-methylsulfanylpyrimidine, 2-(4,6-DMP)-SAA = 2-(4,6-dimethylpyrimidin-2-yl)sulfanylacetamide, MTA = N-(5-methylthiazol-2-yl)acetamide, 1-NAA = 1-naphthylacetic acid, PTU = propylthiouracil, ADPR = adenosine diphosphate ribose, AMP = adenosine monophosphate, statistics (t-test): * $p \leq 0.05$; ** $p \leq 0.005$; *** $p \leq 0.0001$, all compared pairwise to a vehicle (DMSO) control.

screening, we tested fragments of SirReal2 and ADPR to assess their potency to prevent binding of Sirt2 to the immobilized SirReal probe (Figure 3d and Figure S6). As expected, fragments of SirReal2, as well as AMP as a fragment of ADPR, significantly prevented Sirt2 from binding to the probe. We confirmed that methylation of the pyrimidine moiety in positions 4 and 6 is crucial for binding to Sirt2,^[17] since the dimethylated fragment (4,6-DM-2-MSP) provokes a significant decrease in Sirt2 binding compared to the fragment without methyl groups (2-MSP). No effect was observed for the negative control of nicotinamide (NA) and propylthiouracil (PTU), a pyrimidine structurally different from 4,6-DM-2-MSP. Furthermore, we wanted to investigate the suitability of our SirReal probe for affinity purification and pull-down experiments. By using our SirReal probe, we were able to extract Sirt2 selectively out of various complex matrices, even in the presence of the similar Sirt1 or the promiscuous ligand binding protein BSA (bovine serum albumin). We demonstrated this by using a model protein

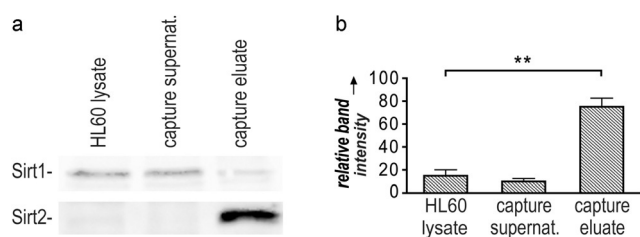


Figure 4. The SirReal probe (11) captures Sirt2 out of HL60 lysates. a) Western blot analysis of the SirReal probe bound to Dynabeads MyOne Streptavidin T1 after incubation with HL60 lysates. Sirt1 and Sirt2 were detected with isotype-specific antibodies (for uncropped blots see Figure S7d,e). b) Quantification of the Western blot analysis. Affinity pull-down experiments lead to a significant enrichment of Sirt2 ($n=3$). Statistics (t-test): ** $p \leq 0.005$

mixture of the three mentioned proteins (Figure S7a), mixtures of *E. coli* lysates where Sirt1 or Sirt2 are overexpressed (Figure S7b,c), and native HL60 lysates (Figure 4 and see Figure S7d,e). The specificity of the pull-down was shown by blocking the Sirt2 enrichment effectively with either biotin or SirReal2 (2, see Figure S7a). These results underline the isotype selectivity, robustness, and broad applicability of our SirReal probe for affinity purification and pull-down experiments.

In this study, we reported the structure-based development of an affinity probe for Sirt2. The design of the probe was guided by the structural insights gained by Sirt2–SirReal cocystal structures and rationalized by molecular docking as well as by the synthesis of druglike probe mimics that extend into the acyllysine tunnel, as shown by X-ray crystallography. These inhibitors displayed an improved potency, enhanced water solubility, and improved efficacy in target engagement compared to the previous lead structure SirReal2. This has important implications for further drug discovery in the field of sirtuin inhibitors. Our new SirReal probe retains the potency and isotype selectivity of the druglike inhibitors and is able to selectively bind to Sirt2 in different matrices. Based on our biophysical data, the key to its strong binding is the slow dissociation rate of the inhibitor–enzyme complex. Slow dissociation rates have been proposed recently as a key step for drug design towards optimized cellular activity^[22] and, for the first time, we have exploited this principle systematically in the structure-guided development of a chemoaffinity probe. This approach lays the foundation for widespread applications such as FBDD, kinetic measurements, and use in inhibitor characterization. Furthermore, our new SirReal probe opens up new avenues to dissect the role of Sirt2 in biology and medicine. Ongoing studies are directed at detecting novel Sirt2 interaction partners by chemoproteomics,^[26] and assessing genome-wide binding profiles of Sirt2 by using Chem-seq.^[27] Our SirReal probe, therefore, represents a highly versatile tool that provides excellent isotype selectivity and high affinity to the target enzyme Sirt2, and can now be used to interrogate Sirt2 biology and druggability on a new level.

Acknowledgements

We thank the Deutsche Forschungsgemeinschaft (DFG) for funding (Ju295/8-1, Si868/6-1, SFB992: A04 & Z02), K. SchmidtKunz for assistance with cell culture experiments, and E. Jung for the preparation of the graphic for the Table of Contents. J.O. was supported by the Hungarian National Scientific Research Fund Grants OTKA T-101039 and T-112144.

Keywords: deacylases · drug design · protein modifications · proteomics · sirtuins

How to cite: *Angew. Chem. Int. Ed.* **2016**, *55*, 2252–2256
Angew. Chem. **2016**, *128*, 2293–2297

- [1] a) S. Imai, C. M. Armstrong, M. Kaeberlein, L. Guarente, *Nature* **2000**, *403*, 795–800; b) A. Vaquero, M. B. Scher, D. H. Lee, A. Sutton, H. L. Cheng, F. W. Alt, L. Serrano, R. Sternglanz, D. Reinberg, *Genes Dev.* **2006**, *20*, 1256–1261.
- [2] H. Vaziri, S. K. Dessain, E. N. Eaton, S. I. Imai, R. A. Frye, T. K. Pandita, L. Guarente, R. A. Weinberg, *Cell* **2001**, *107*, 149–159.
- [3] F. Yeung, J. E. Hoberg, C. S. Ramsey, M. D. Keller, D. R. Jones, R. A. Frye, M. W. Mayo, *EMBO J.* **2004**, *23*, 2369–2380.
- [4] B. J. North, B. L. Marshall, M. T. Borra, J. M. Denu, E. Verdin, *Mol. Cell* **2003**, *11*, 437–444.
- [5] B. J. North, M. A. Rosenberg, K. B. Jeganathan, A. V. Hafner, S. Michan, J. Dai, D. J. Baker, Y. Cen, L. E. Wu, A. A. Sauve, J. M. van Deursen, A. Rosenzweig, D. A. Sinclair, *EMBO J.* **2014**, *33*, 1438–1453.
- [6] J. L. Feldman, J. Baeza, J. M. Denu, *J. Biol. Chem.* **2013**, *288*, 31350–31356.
- [7] J. Du, Y. Zhou, X. Su, J. J. Yu, S. Khan, H. Jiang, J. Kim, J. Woo, J. H. Kim, B. H. Choi, B. He, W. Chen, S. Zhang, R. A. Cerione, J. Auwerx, Q. Hao, H. Lin, *Science* **2011**, *334*, 806–809.
- [8] J. Du, H. Jiang, H. Lin, *Biochemistry* **2009**, *48*, 2878–2890.
- [9] J. Schemies, U. Uciechowska, W. Sippl, M. Jung, *Med. Res. Rev.* **2010**, *30*, 861–889.
- [10] R. M. de Oliveira, J. Sarkander, A. G. Kazantsev, T. F. Outeiro, *Front. Pharmacol.* **2012**, *3*, 82.
- [11] B. Beirowski, J. Gustin, S. M. Armour, H. Yamamoto, A. Viader, B. J. North, S. Michan, R. H. Baloh, J. P. Golden, R. E. Schmidt, D. A. Sinclair, J. Auwerx, J. Milbrandt, *Proc. Natl. Acad. Sci. USA* **2011**, *108*, E952–961.
- [12] T. F. Pais, E. M. Szego, O. Marques, L. Miller-Fleming, P. Antas, P. Guerreiro, R. M. de Oliveira, B. Kasapoglu, T. F. Outeiro, *EMBO J.* **2013**, *32*, 2603–2616.
- [13] a) H. S. Kim, A. Vassilopoulos, R. H. Wang, T. Lahusen, Z. Xiao, X. Xu, C. Li, T. D. Veenstra, B. Li, H. Yu, J. Ji, X. W. Wang, S. H. Park, Y. I. Cha, D. Gius, C. X. Deng, *Cancer Cell* **2011**, *20*, 487–499; b) L. Serrano, P. Martinez-Redondo, A. Marazuela-Duque, B. N. Vazquez, S. J. Dooley, P. Voigt, D. B. Beck, N. Kane-Goldsmith, Q. Tong, R. M. Rabanal, D. Fondevila, P. Munoz, M. Kruger, J. A. Tischfield, A. Vaquero, *Genes Dev.* **2013**, *27*, 639–653.
- [14] a) M. H. Yang, G. Laurent, A. S. Bause, R. Spang, N. German, M. C. Haigis, K. M. Haigis, *Mol. Cancer Res.* **2013**, *11*, 1072–1077; b) P. Y. Liu, N. Xu, A. Malyukova, C. J. Scarlett, Y. T. Sun, X. D. Zhang, D. Ling, S. P. Su, C. Nelson, D. K. Chang, J. Koach, A. E. Tee, M. Haber, M. D. Norris, C. Toon, I. Rومان, C. Xue, B. B. Cheung, S. Kumar, G. M. Marshall, A. V. Biankin, T. Liu, *Cell Death Differ.* **2013**, *20*, 503–514.
- [15] H. A. Eskandarian, F. Impens, M. A. Nahori, G. Soubigou, J. Y. Coppee, P. Cossart, M. A. Hamon, *Science* **2013**, *341*, 1238858.

- [16] a) J. S. Disch, G. Evindar, C. H. Chiu, C. A. Blum, H. Dai, L. Jin, E. Schuman, K. E. Lind, S. L. Belyanskaya, J. Deng, F. Coppo, L. Aquilani, T. L. Graybill, J. W. Cuzzo, S. Lavu, C. Mao, G. P. Vlasuk, R. B. Perni, *J. Med. Chem.* **2013**, *56*, 3666–3679; b) H. Cui, Z. Kamal, T. Ai, Y. Xu, S. S. More, D. J. Wilson, L. Chen, *J. Med. Chem.* **2014**, *57*, 8340–8357; c) K. Yamagata, Y. Goto, H. Nishimasu, J. Morimoto, R. Ishitani, N. Dohmae, N. Takeda, R. Nagai, I. Komuro, H. Suga, O. Nureki, *Structure* **2014**, *22*, 345–352.
- [17] T. Rumpf, M. Schiedel, B. Karaman, C. Roessler, B. J. North, A. Lehotzky, J. Olah, K. I. Ladwein, K. Schmidtkunz, M. Gajer, M. Pannek, C. Steegborn, D. A. Sinclair, S. Gerhardt, J. Ovadi, M. Schutkowski, W. Sippl, O. Einsle, M. Jung, *Nat. Commun.* **2015**, *6*, 6263.
- [18] a) D. Urankar, J. Kosmrlj, *J. Comb. Chem.* **2008**, *10*, 981–985; b) M. Krasavin, R. Karapetian, I. Konstantinov, Y. Gezentsvey, K. Bukhryakov, E. Godovykh, O. Soldatkina, Y. Lavrovsky, A. V. Sosnov, A. A. Gakh, *Arch. Pharm.* **2009**, *342*, 420–427; c) N. D. Obushak, V. S. Matiichuk, R. Y. Vasylyshin, Y. V. Ostapyuk, *Russ. J. Org. Chem.* **2004**, *40*, 383–389.
- [19] S. I. Zav'yalov, N. E. Kravchenko, G. I. Ezhova, L. B. Kulikova, A. G. Zavozin, O. V. Dorofeeva, *Pharm. Chem. J.* **2007**, *41*, 105–108.
- [20] a) R. Huisgen, *Proc. Chem. Soc. London* **1961**, 357–396; b) T. R. Chan, R. Hilgraf, K. B. Sharpless, V. V. Fokin, *Org. Lett.* **2004**, *6*, 2853–2855.
- [21] B. Heltweg, J. Trapp, M. Jung, *Methods* **2005**, *36*, 332–337.
- [22] A. Basavapathruni, L. Jin, S. R. Daigle, C. R. Majer, C. A. Therkelsen, T. J. Wigle, K. W. Kuntz, R. Chesworth, R. M. Pollock, M. P. Scott, M. P. Moyer, V. M. Richon, R. A. Copeland, E. J. Olhava, *Chem. Biol. Drug Des.* **2012**, *80*, 971–980.
- [23] Y. N. Cen, J. N. Falco, P. Xu, D. Y. Youn, A. A. Sauve, *Org. Biomol. Chem.* **2011**, *9*, 987–993.
- [24] J. Schiebel, N. Radeva, H. Koster, A. Metz, T. Krotzky, M. Kuhnert, W. E. Diederich, A. Heine, L. Neumann, C. Atmanene, D. Roecklin, V. Vivat-Hannah, J. P. Renaud, R. Meinecke, N. Schlinck, A. Sitte, F. Popp, M. Zeeb, G. Klebe, *ChemMedChem* **2015**, *10*, 1511–1521.
- [25] R. J. Hall, P. N. Mortenson, C. W. Murray, *Prog. Biophys. Mol. Biol.* **2014**, *116*, 82–91.
- [26] M. Bantscheff, G. Drewes, *Bioorg. Med. Chem.* **2012**, *20*, 1973–1978.
- [27] L. Anders, M. G. Guenther, J. Qi, Z. P. Fan, J. J. Marineau, P. B. Rahl, J. Loven, A. A. Sigova, W. B. Smith, T. I. Lee, J. E. Bradner, R. A. Young, *Nat. Biotechnol.* **2014**, *32*, 92–96.

Received: October 21, 2015

Published online: January 8, 2016